International Conference on Space Optics—ICSO 2018

Chania, Greece

9–12 October 2018

Edited by Zoran Sodnik, Nikos Karafolas, and Bruno Cugny

Towards a tilt-to-length coupling calibration on the GRACE follow-on laser ranging instrument

H. Wegener

International Conference on Space Optics — ICSO 2018, edited by Zoran Sodnik, Nikos Karafolas, Bruno Cugny, Proc. of SPIE Vol. 11180, 1118047 · © 2018 ESA and CNES · CCC code: 0277-786X/18/$18 · doi: 10.1117/12.2536070

Towards a Tilt-to-Length Coupling Calibration on the GRACE Follow-On Laser Ranging Instrument

H. Wegener[a,*] on behalf of the LRI team

[a]Max Planck Institute for Gravitational Physics (Albert Einstein Institute) and Institute for Gravitational Physics, Leibniz Universität Hannover, Callinstr. 38, 30167 Hannover, Germany

[*]henry.wegener@aei.mpg.de

ABSTRACT

The Laser Ranging Instrument (LRI) measures the biased range between the two GRACE Follow-On spacecraft (launched in May 2018) using laser interferometry. It is the first of its type and serves as a technology demonstrator. Here we present the working principle and a brief report on the first turn-on of the instrument. In particular, we will discuss the laser link acquisition and possible methods of calibrating Tilt-to-Length coupling.

Keywords: LRI, GRACE Follow-On, Gravity Field, Laser Interferometry, Inter-Satellite Ranging

1. INTRODUCTION

The GRACE Follow-On (GFO) mission was successfully launched on 22 May 2018. Its goal is to continue the extremely valuable measurements of the Gravity Recovery and Climate Experiment (GRACE) mission[1] (2002-2017). The main science measurement on both missions is the inter-satellite biased range, measured by the K-Band Ranging (KBR) instrument. In addition, the GFO spacecraft carry the innovative Laser Ranging Instrument (LRI) as a technology demonstrator[2], which is designed to provide in principle the same observable as the KBR, but with the potential of lower instrument noise.

The LRI was turned on for the first time in June 2018, less than 4 weeks after launch. It is the first laser interferometer measuring inter-satellite distances ever operated in space - following the first laser interferometer in space on LISA Pathfinder[3]. After the LRI was switched on, it performed a pre-programmed acquisition scan[4], using its fast steering mirrors (FSM). This initial scan was successful on first attempt, and the LRI immediately started to gather range data.

This paper is meant to give a brief and non-exhaustive report on the working principle of the LRI and its subsystems. At the time of writing, the commissioning phase of the GFO mission is ongoing. Detailed results will be published by the LRI team soon. Here we will explain the laser link acquisition strategy, the spacecraft attitude determination via Differential Wavefront Sensing (DWS) technique, and the ranging noise contributions. In particular, the ranging noise due to spacecraft pointing jitter (called Tilt-to-Length (TTL) coupling) and possible methods of calibrating it will be discussed.

2. LRI WORKING PRINCIPLE

Ranging measurement principle

The LRI is an optical interferometer, which is operated with a near-IR wavelength of 1064nm and where the optical layout is arranged in a race-track configuration as shown in fig. 1. The direction of laser beams is reversed on each S/C by an approx. 60 cm long triple-mirror assembly (TMA), utilizing three mutual perpendicular mirrors in a corner-cube arrangement. The vertex of the TMA is co-located with the accelerometer and S/C center-of-mass (CoM) in order to minimize to a large extent the tilt-to-length coupling. The lateral separation of 60 cm between in-coming and out-going beam was required due to space constraints on the S/C, i.e. the central axis between the CoM is occupied by the KBR instrument and by cold-gas tanks. This spatial separation of beams has the advantage that one can relinquish polarization

multiplexing as usually present in single-axis interferometers, which reduces the number of optical components and the complexity of the interferometer.

The LRI is a heterodyne interferometer designed for phase-tracking of beatnote frequencies between 4..16 MHz, which are produced by the interference of optical fields with the MHz difference in optical frequency. Both S/C accommodate identical optical bench assemblies (OBA), which are connected by optical fibers to the NPRO laser with 25 mW output power. The laser light is guided over a two-axis fast steering mirror (FSM) onto the recombination beamsplitter (RBS, fig. 1). A small fraction of the light is transmitted at the RBS towards some imaging optics and the hot-redundant quadrant phtotodiodes (QPD, fig. 1), while most of the laser light leaves the OBA towards the TMA. The TMA retro-reflects the beam with approx. 2.5 mm 1/e² radius and 20 mW optical power in the direction of the distant S/C. The laser light expands to a diameter of over 50 meter and gains a Doppler shift (w.r.t. the receiver craft) while traveling the 220 km distance. This Doppler frequency shift contains the ranging information, which is read out by the phase measurements.

Only a small fraction of the expanded laser beam is cut out by the 8 mm diameter receiving aperture on the OBA, yielding an optical power of less than 2 nW on the OBA to be interfered with the local laser beam. In principle, both OBAs obtain Doppler shifted laser light and measure the phase of the received light w.r.t. to the local laser. However, the LRI is operated in a transponder scheme, where one satellite is designated as slave with an active frequency-offset phase-locked loop. This control loop actuates with high gain and high bandwidth the NPRO laser phase so that a constant phase ramp with a slope of 10 MHz is measured by the phasemeter on the slave S/C. This means that the phase of the local laser is locked to the incoming phase and the phase information is transported on the laser light to the master S/C. The master side measures twice, or the round-trip, Doppler shift in addition to the frequency-offset imprinted by the slave, while the slave satellite measures a trivial constant phase ramp due to the frequency-offset.

The master side exhibits an active laser frequency stabilization by means of an ULE optical cavity[5] in order to minimize phase fluctuations, which couple via the round-trip propagation into the final phase measurement on the master side. Since the frequency stabilization and the optical cavity are present on both S/C, the master and slave role is interchangeable between the S/C yielding additional redundancy.

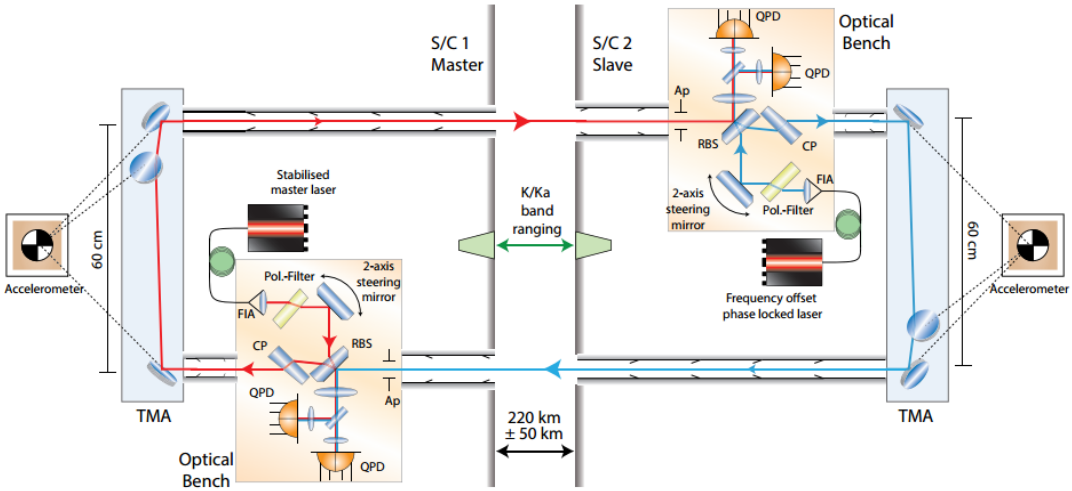

Figure 1. Sketch of the LRI measurement principle. Image credit: Vitali Müller / AEI Hannover

Laser beam steering

The LRI requires accurate pointing of the transmit laser beam, which has a 1/e² half-angle divergence of approx. 140 µrad, in order to transmit a sufficient amount of light power to the other S/C. Since the S/C pointing uncertainty and attitude variations are much larger than the LRI pointing requirements, active beam steering is employed by means of control loops and fast steering mirrors (FSM). Therefore, quadrant photodiodes (QPD) measure the tip and tilt of the local beam with respect to the incoming beam, using the differential wavefront sensing (DWS) technique[6,7]. This principle is depicted in fig. 2. This DWS signal is fed back to the control loop, commanding the steering mirror in such a way that the DWS signal is driven towards a programmed set point. In an ideal scenario (with perfect component

placement and alignment), this set point is zero and both phasefronts are parallel in front of the QPDs as long as the local S/C misalignment is within the range of the optics and steering mirror. The FSM control loop compensates for misalignments of the local S/C and ensures that the heterodyne efficency and corresponding signal-to-noise ratio of the phase readout is maximized. With a closed control loop and zero DWS set point, the incoming phasefront is parallel to the outgoing phasefronts on the OBA, which means that after retro-reflection at the TMA, the emitted light is propagating in the direction of the received light and towards the distant S/C.

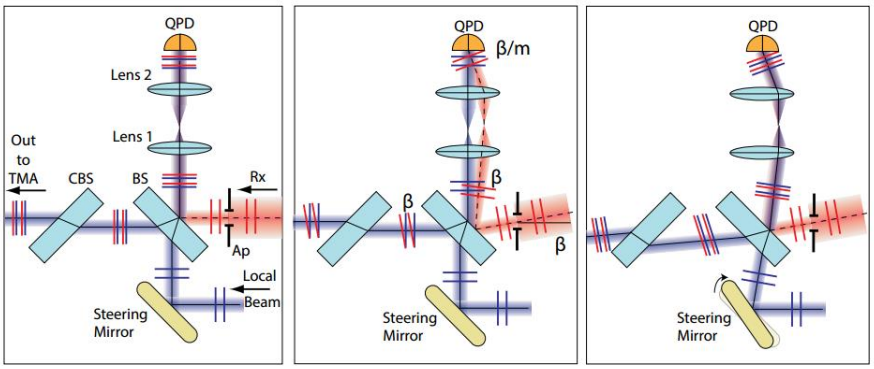

Figure 2. Working principle of DWS and FSM. Image credit: Vitali Müller / AEI Hannover

Pointing angle measurement

Since the FSM is permanently commanded to compensate for the misalignment of the received light field and the local laser beam, the FSM positions provide very accurate information about the alignment of the spacecraft with respect to the line of sight (LoS), and hence about the spacecraft LoS pointing angles. This method directly measures the pointing angles, i.e. the deviation of the local frame from the line-of-sight frame. As opposed to that, other attitude sensors (e.g. Star Cameras) measure the satellites' attitudes compared to inertial space, which can be combined with orbit data in order to obtain pointing angles. However, the LRI does not measure the spacecraft roll angle (which is the angle around the satellites' line-of-sight), only the vertical and horizontal angles which correspond to the so-called pitch and yaw angles.

3. LASER LINK ACQUISITION

Initial acquisition strategy

The LRI has a field-of-view of plus-minus a few milliradians, which is designed to be larger than the pointing variations of the satellites and initial uncertainties, e.g. due to alignment tolerances during instrument integration. It is however required to perform a search within this field-of-view, in order to close the interferometric link. This pointing offset, which is unknown initially, has to be determined in-flight. Furthermore, the laser frequency difference between master and slave is required to be in the measurable range of 4..16 MHz. To this end, an initial acquisition scan is performed on both spacecraft simultaneously ("initial line of sight calibration procedure"[4]). Afterwards, the pointing offset is determined from the steering mirror positions recorded at the instances when the phasemeter detects flashes, i.e. when the beatnote amplitude exceeds a threshold. These split-second flashes are seen only if all of the 4 angles (pitch and yaw for both spacecraft) and laser frequency offset are very close to their optimal values at the same time. Thus, a complicated five-dimensional scan pattern is needed, which is depicted in fig. 3 for the angular domain. The total duration of the scan is approximately nine hours. During this initial acquisition scan there is no transition into science mode. The data is merely recorded and analyzed afterwards. When the optimal set point is determined, a parameter file is uploaded to the spacecraft.

Once the initial pointing offsets are uploaded, the LRI is commanded into the re-acquisition mode. In this mode, the instrument performs only a short scan with smaller range, starting with the values that were previously determined by the initial line of sight calibration procedure. These values are already very close to the optimum and the instrument

automatically attempts to transition from the re-acquisition mode into the science mode, once a re-acquisition flash is seen.

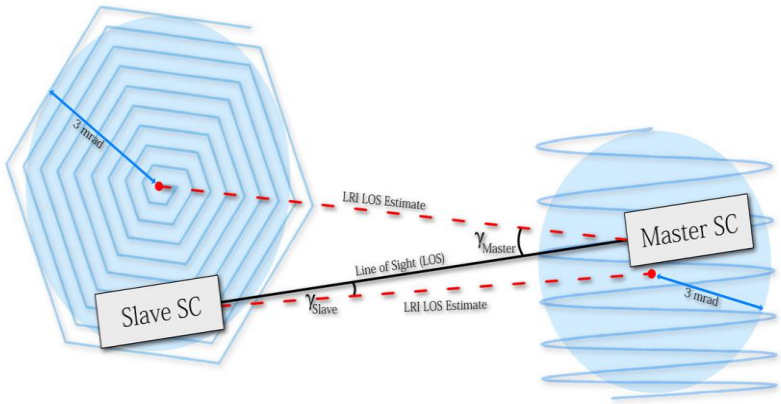

Figure 3. Schematic of the LRI initial acquisition scan. Image credit: Alexander Koch / AEI Hannover

Result

This initial acquisition scan was performed on 13 June 2018. The data recorded during the scan was sent to ground and analyzed the following night. The analysis showed that enough flashes were recorded in order to determine the initial offsets for the re-acquisition scan, which include the major misalignment of the LRI OBA w.r.t. the satellite frame (SF) and the minor TMA co-alignment error and estimation errors in the pointing towards the distant spacecraft. The parameter files containing this information were uploaded shortly afterwards. The same day, the instrument successfully established the interferometer laser link. The following ground-station pass of the satellites confirmed that the LRI was in science mode and taking continuous measurements.

4. TILT-TO-LENGTH (TTL) COUPLING

TMA vertex point offset

One of the expected error sources in the LRI ranging measurements is the TTL coupling, i.e. the ranging error which is caused by spacecraft attitude variations. A main reason for this is an offset between the satellite CoM and the so-called vertex point (VP) of the TMA, which is the virtual intersection point of the three mirrors[8]. One of the advantages of the LRI concept is that the interferometer round-trip length is exactly two times the distance from VP to VP. This implies that the measured range is independent of rotations around those points. However, rotations around a different point change the position of the VP which then causes undesired variations in the ranging measurement.

TTL calibration

A mathematical derivation of the known TTL coupling effects indicate that a model which is linear in the pointing angles can be used to explain the main part of the TTL error. That is, we assume that each of the 6 pointing angles (roll, pitch, yaw for each of the two spacecraft) linearly adds to the ranging measurement, weighted by a coupling factor. Since the attitudes of the satellites are known quite accurately, this error can in theory be computed and subtracted from the measured range, if the 6 coupling factors can be estimated well enough.

One possible way to estimate the TTL coupling factors is to use a dedicated satellite rotation maneuver, i.e. commanding the satellite AOCS to produce periodic pointing angle oscillations. Similar approaches are used for the calibration of the KBR instrument and for the accelerometer calibration. The KBR calibration maneuvers cannot be used for this purpose, since it uses angle amplitudes which are too large for the LRI to cope with. The goal of the accelerometer calibration or "center-of-mass calibration" (CMC) maneuver is to determine the offset between the CoM of the satellite and the CoM of the accelerometer proof mass[9]. A CMC maneuver consists of small periodic pointing angle excitations for a duration

of 180 seconds. The oscillation period is 12 seconds, which corresponds to 83.3 mHz. These calibration maneuvers, which are planned to be performed regularly, could be useful for the LRI as well. If needed, the maneuver parameters can also be adjusted to values that are optimal for the purpose of LRI TTL calibration.

Another possible strategy is to use the naturally occuring pointing variations of the satellites. The advantage of this approach is that it requires merely the regular data stream, which is typically available for long durations without large gaps. On the other hand, the data analysis in this case is more complex. The ranging signal in lower frequencies is dominated by the gravity signal, which has to be carefully subtracted beforehand. In higher frequencies, the pointing variations are very small, so that the TTL error signal is expected to be buried by other noise sources and especially hard to detect.

In either case, the first step is to prepare a data set of 6 pointing angles and a quantity that contains the TTL error, which is either directly the measured range or derived from it (e.g. post-fit residuals). The data is synchronized and bandpass filtered. TTL coupling factors can be estimated by using linear least-squares, i.e. by minimizing the expression

$$\left(y - \sum_{i=1}^{6} c_i x_i\right)^T \cdot \left(y - \sum_{i=1}^{6} c_i x_i\right)$$

where x_i, i=1,…,6, are the pointing angles, c_i are the coupling factors, and y is the range or range-derived quantity. This procedure can be improved by using advanced formalisms, where additional information (e.g. knowledge about instrument noise) can be taken into account. The analysis is ongoing and detailed results will be published when they are available.

5. INSTRUMENT OPERATION

Proof-of-concept

After the LRI had started taking range data on 14 June 2018, it has proven that it can take measurements for many orbits without any interruptions. A good opportunity for a first test of the ranging data came up when the GFO satellites were flying over the Himalayas. After highpass filtering, the ranging data clearly shows a signal that is caused by change in the inter-spacecraft separation due to the presence of the large mass of the Himalayas. This proof-of-concept visualization shown in fig. 4 is hence called “Himalaya Plot”. Fig. 4 was originally published on the AEI Hannover web page[10], a similar plot was published at the same time on the JPL web page[11]. Likewise, a Himalaya plot for the GFO KBR instrument[12] can be found on the NASA web page[12].

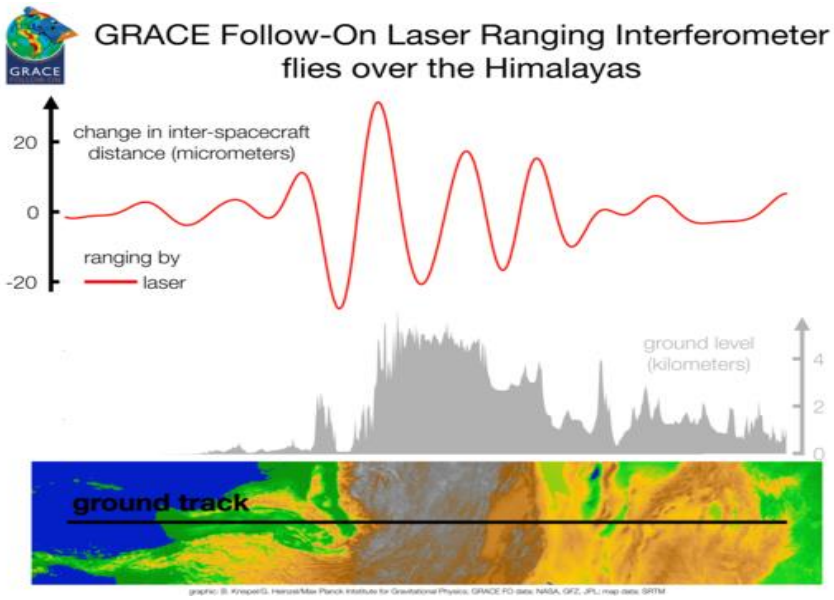

Figure 4. “Himalaya Plot”. Top: LRI ranging data measured as the satellites flew over the Himalayas. Middle and bottom: Topography of the ground track (source: SRTM). Image credit: Gerhard Heinzel / AEI Hannover

6. SUMMARY

The LRI has proven its functionality to measure inter-satellite biased range in orbit. The initial acquisition scan has been successful and the laser link between the two spacecraft could be established on first attempt. The DWS control loop is working as expected and the steering mirrors are able to control the beam direction towards the distant spacecraft. The mission is in the commissioning phase and detailed analysis of the instrument noise is ongoing. The final conclusions, including ranging performance and performance of the attitude determination (pitch and yaw), will be published after the ending of the commissioning.

ACKNOWLEDGEMENTS

The LRI is jointly managed by NASA Jet Propulsion Laboratory, California Institute of Technology, Pasadena, California, USA, and the Max Planck Institute for Gravitational Physics (Albert Einstein Institute) in Hannover, Germany. This work is presented on behalf of the LRI team. The work at AEI Hannover is supported by funding from the Bundesministerium für Bildung und Forschung (BMBF) under the support code (“Förderkennzeichen”) FKZ 03F0654B. The author is responsible for the content of this article.
The author would like to thank the DFG Sonderforschungsbereich (SFB) 1128 Relativistic Geodesy and Gravimetry with Quantum Sensors (geo-Q) for financial support.
GRACE-FO is a partnership between NASA and German Research Centre for Geosciences in Potsdam, Germany. JPL manages the mission for NASA's Science Mission Directorate. Additional contributors to the LRI include SpaceTech in Immenstaad, Germany; Tesat-Spacecom in Backnang, Germany; Ball Aerospace in Boulder, Colorado; iXblue in Saint-Germain-en-Laye, France; the German Aerospace Center (DLR) Institute of Robotics and Mechatronics in Adlershof and Institute of Space Systems in Bremen; Hensoldt Optronics in Oberkochen; Apcon AeroSpace and Defence in Neubiberg/Munich; Diamond USA, Inc., and Diamond SA in Losone, Switzerland; Airbus Defence and Space in Friedrichshafen; and The Australian National University.

REFERENCES

[1] Tapley, B. D., et al, "The Gravity Recovery and Climate Experiment: Mission Overview and Early Results," Gephysical Research Letters 31 (2004).
[2] Sheard, B. S., Heinzel, G., Danzmann, K., Shaddock, D. A., Klipstein, W. M. and Folkner, W. M., "Intersatellite Laser Ranging Instrument for the GRACE Follow-On Mission," Journal of Geodesy 86(12), 1083-1095 (2012).
[3] Armano, M., et al, "Sub-Femto-g Free Fall for Space-Based Gravitational Wave Observatories: LISA Pathfinder Results," Physical Review Letters 116 (2016).
[4] Koch, A., et al, "Line of Sight Calibration for the Laser Ranging Interferometer on-board the GRACE Follow-On Mission: on-ground Experimental Validation," Optical Society of America 1(2), 345-678 (2018).
[5] Thompson, R., et al, "A flight-like Optical Reference Cavity for GRACE Follow-On Laser Frequency Stabilization," 2011 Joint Conference of the IEEE International Frequency Control and the Earopean Frequency and Time Forum (FCS) Proceedings, 1-3 (2011).
[6] Morrison, E., et al, "Automatic Alignment of Optical Interferometers," Appl. Opt. 33, 5041-5049 (1994).
[7] Anderson, D. Z., "Alignment of Resonant Optical Cavities," Appl. Opt. 23, 2944-2949 (1984).
[8] Schütze, D., et al, "Retroreflector for GRACE Follow-On: Vertex vs. Point of Minimal Coupling," Optical Society of America (2014).
[9] Wang, F., et al, "Determination of Center-of-Mass of Gravity Recovery and Climate Experiment Satellites," Journal of Spacecraft and Rockets (2010).
[10] Knispel, B., "First Light for GRACE Follow-On Laser Interferometer," AEI Hannover, http://www.aei.mpg.de/2277280/first-light-for-grace-follow-on-laser-interferometer (2 July 2018).
[11] Buis, A. and Smith, E., "First Laser Light for GRACE Follow-On," NASA JPL, https://www.jpl.nasa.gov/news/news.php?feature=7182 (2 July 2018).
[12] Buis, A., "GRACE-FO Turns on 'Range Finder', Sees Mountain Effects," NASA JPL, https://www.nasa.gov/feature/jpl/grace-fo-turns-on-range-finder-sees-mountain-effects (11 June 2018).
[13] Darbeheshti, N., et al, "Instrument Data Simulations for GRACE Follow-On: Observation and Noise Models," Earth Syst. Sci. Data 9, 833-848 (2017).
[14] Wuchenich, D., et al, "Laser Link Acquisition Demonstration for the GRACE Follow-On Mission," Optics Express 22(9), 11351-11366 (2014).
[15] Flechtner, F., et al, "What can be Expected from the GRACE-FO Laser Ranging Interferometer for Earth Science Applications?," Surv Geo